Journal of Animal Environment

(E-ISSN 2717-1396, ISSN 2717-1388)

Original Research Paper

Phytochemical Standardization and Neuroprotective Potential of *Celastrus paniculatus* Seed Extract Against Amyloid-β-Induced Neuronal Injury: Insights into Oxidative and Cholinergic Dysfunction

[1]Rajapandi Raju, [2]Basu Venkateswara Reddy, [3]Neelmani Chauhan*, [4]Mohan Verma, [5]Zufnoon Khan, [6]Amrita Thakur, [7]Avinash S Jiddewar, [8]Erigi Nikhil Chakravarthy

[1]Professor, School of Pharmacy, SBV Karaikal Campus, Sri Balaji Vidyapeeth (Deemed to be University) Puducherry. 609 609

[2]Professor and Head, Department of Pharmaceutics, Srinivasa Institute of Pharmaceutical Sciences, Pedda Settipalli, Proddutur, Kadapa. 516361

[3]Associate Professor, Technocrates Institute of Technology, Department of Pharmacy, Bhopal, Madhya Pradesh.

[4]Assistant Professor, Department of Pharmaceutical Sciences, Central University of Haryana, Mahendergarh. 123031

[5]Assistant Professor, Department of Pharmacy -IBMER, Mangalayatan University Aligarh-202146, India

[6]Department of Pharmaceutics, Vishwakarma University, Pune, Maharashtra.

[7]Principal, NSPM College of Pharmacy, Darwha, Yavatmal.

[8]Associate Professor, Department of Pharmacology, Teegala Krishna Reddy College of Pharmacy, Medbowli, Meerpet, Balapur Mandal, Ranga Reddy, Hyderabad, Telangana. 500097

Corresponding Author: [3]Neelmani Chauhan
Email: neel710@gmail.com

Abstract:
Celastrus paniculatus has traditionally been associated with cognitive and neurological benefits; however, integration of phytochemical standardization with mechanistic evaluation of its neuroprotective activity remains important. This study investigated the phytochemical characteristics, antioxidant activity, acetylcholinesterase (AChE) inhibition, and neuroprotective potential of a hydroalcoholic extract of *C. paniculatus* seeds (CPHE) against amyloid-β1–42 (Aβ1–42)-induced injury in differentiated SH-SY5Y cells. CPHE showed an extraction yield of 12.74% and contained 68.42 ± 2.31 mg GAE/g total phenolics and 31.76 ± 1.48 mg QE/g total flavonoids. HPLC-PDA analysis provided a characteristic multicomponent fingerprint. CPHE exhibited concentration-dependent DPPH and ABTS radical-scavenging activities, with IC50 values of 61.8 and 50.7 µg/mL, respectively, and inhibited AChE with an IC50 of approximately 70 µg/mL. Aβ1–42 exposure reduced neuronal cell viability to 65.6 ± 2.8%, whereas CPHE increased viability dose-dependently to 90.4 ± 2.3% at 100 µg/mL. CPHE also attenuated intracellular reactive oxygen species and cellular AChE activity while restoring superoxide dismutase, catalase, and reduced glutathione levels. These findings

***Corresponding Author:**
Received: 25th July, 2026 | Revised: 26th August, 2026 | Accepted: 18th September, 2026 | Available Online: 24th September, 2026
(DOI): 10.70102/AEJ.2026.18.7s.42

demonstrate that standardized CPHE provides significant in vitro neuroprotection against Aβ1–42-induced neuronal injury, associated with complementary antioxidant and cholinesterase-modulating activities.

Keywords: *Celastrus paniculatus*; amyloid-β1–42; neuroprotection; acetylcholinesterase; oxidative stress; SH-SY5Y cells; phytochemical standardization

1. Introduction

Alzheimer's disease (AD) is a progressive neurodegenerative disorder and a major cause of dementia, characterized clinically by deterioration of memory, learning, executive function, and other cognitive abilities. Its pathogenesis is multifactorial and involves interconnected abnormalities including extracellular accumulation of amyloid-β (Aβ) peptides, tau-associated pathology, synaptic dysfunction, oxidative stress, neuroinflammation, mitochondrial impairment, and progressive neuronal loss. Among these alterations, disruption of cholinergic neurotransmission and oxidative homeostasis represents an important component of cognitive dysfunction. The complexity of these interacting mechanisms has also highlighted the limitations of therapeutic approaches directed toward a single pathological process (Katramadou et al., 2026; Kwon & Lee, 2025; Schwarthoff et al., 2021; Shcheblykina et al., 2026).

Cholinergic dysfunction is strongly associated with cognitive impairment in AD. Degeneration of cholinergic neurons and reduced availability of acetylcholine can compromise neuronal communication involved in learning and memory. Acetylcholinesterase (AChE), the enzyme responsible for hydrolysis of acetylcholine within cholinergic synapses, consequently represents an established pharmacological target. AChE inhibitors such as donepezil can enhance cholinergic neurotransmission and provide symptomatic benefit in patients with AD. Nevertheless, cholinesterase inhibition alone does not adequately address the multiple cellular processes contributing to progressive neurodegeneration. Identification of agents combining cholinesterase-modulating activity with complementary neuroprotective properties therefore remains pharmacologically relevant (Asken et al., 2025; Bayraktaroglu et al., 2025; Favari & Parolini, 2025; Marques & Campos, 2024; Qian et al., 2026).

Oxidative stress constitutes another important feature of AD-associated neuronal injury. The brain is particularly susceptible to oxidative damage because of its high oxygen consumption, abundance of oxidation-sensitive lipids, and substantial metabolic activity. Aβ-associated cellular stress can promote excessive generation of reactive oxygen species (ROS), resulting in oxidative modification of cellular macromolecules and disruption of neuronal homeostasis. Endogenous protective systems, including superoxide dismutase (SOD), catalase (CAT), and reduced glutathione (GSH), normally limit oxidative injury. Disturbance of these defences can intensify oxidative damage and increase neuronal vulnerability. Accordingly, compounds capable of reducing intracellular oxidative stress while preserving endogenous antioxidant defences may provide complementary neuroprotective effects (Katramadou et al., 2026; Rodkin et al., 2026; Zhao & He, 2025).

Medicinal plants constitute chemically diverse sources of bioactive molecules capable of influencing multiple biological targets. *Celastrus paniculatus* Willd., belonging to the family Celastraceae, is a medicinal plant traditionally valued in South Asian systems of medicine, particularly for preparations associated with memory and cognitive function. Its seeds and seed-derived preparations have attracted pharmacological interest because of reported nootropic, antioxidant, and neuropharmacological properties. Phytochemical investigations indicate that *C. paniculatus* seeds contain chemically

diverse constituents, including terpenoid and steroidal constituents as well as phenolic and other secondary metabolites. Such chemical complexity may permit complementary pharmacological actions rather than activity through a single molecular target (Kumar & Jaitak, 2026; Mali et al., 2026; Phattanakiatsakul et al., 2024; Ralta et al., 2023; Satam et al., 2025; Thongon et al., 2026).

Despite this therapeutic interest, interpretation of botanical neuropharmacology is frequently complicated by inadequate chemical standardization of extracts. Differences in plant source, processing, extraction solvent, and analytical methodology can substantially alter phytochemical composition and consequently biological activity. Integration of quantitative phytochemical assessment with chromatographic fingerprinting is therefore essential for establishing the identity and reproducibility of the extract subjected to biological evaluation. Furthermore, antioxidant activity demonstrated exclusively by cell-free radical-scavenging assays cannot by itself establish neuronal protection. Biological relevance is strengthened when chemical antioxidant activity is supported by evidence from a neuronal injury model and corresponding cellular biochemical endpoints (Aleem, 2023; Dwivedi et al., 2026; Manoharan et al., 2025; Satam et al., 2025). Aβ1-42-induced injury in differentiated SH-SY5Y neuronal cells provides a useful in vitro platform for investigating amyloid-associated oxidative and cellular dysfunction. Accordingly, the present study aimed to prepare and phytochemically standardize a hydroalcoholic extract of *C. paniculatus* seeds (CPHE) and evaluate its antioxidant and AChE-inhibitory activities. Its neuroprotective potential was subsequently investigated against Aβ1-42-induced injury in differentiated SH-SY5Y cells by assessing cell viability, intracellular ROS generation, cellular AChE activity, and endogenous antioxidant defences represented by SOD, CAT, and GSH. This integrated approach was designed to determine whether the phytochemically characterized extract exhibits neuroprotective activity associated with attenuation of oxidative stress and cholinergic dysfunction.

2. Materials and Methods

2.1 Plant Material and Authentication

Mature seeds of *Celastrus paniculatus* Willd. were procured from an authenticated herbal raw-material supplier (Angel Herbs). The seeds were examined to remove foreign matter and damaged material and were authenticated on the basis of their taxonomic and pharmacognostic characteristics by a qualified botanist. A voucher specimen was deposited in the institutional herbarium for future reference. The authenticated seeds were cleaned, air-dried under shade where necessary, and coarsely powdered using a mechanical grinder. The powdered material was stored in an airtight, light-resistant container until extraction.

2.2 Chemicals and Reagents

Ethanol, methanol, aluminium chloride, sodium carbonate, Folin–Ciocalteu reagent, gallic acid, quercetin, 2,2-diphenyl-1-picrylhydrazyl (DPPH), 2,2′-azino-bis(3-ethylbenzothiazoline-6-sulfonic acid) diammonium salt (ABTS), potassium persulfate, acetylthiocholine iodide, 5,5′-dithiobis(2-nitrobenzoic acid) (DTNB), and other analytical-grade chemicals were obtained from standard commercial suppliers. Donepezil was used as the reference inhibitor for the acetylcholinesterase assay. Human SH-SY5Y neuroblastoma cells, Dulbecco's Modified Eagle Medium/Ham's F-12 nutrient mixture (DMEM/F-12), fetal bovine serum (FBS), penicillin-streptomycin, phosphate-buffered saline (PBS), trypsin-EDTA, all-trans-retinoic acid, MTT reagent, dimethyl sulfoxide (DMSO), 2′,7′-dichlorodihydrofluorescein diacetate (DCFH-DA), amyloid-β1–42 (Aβ1–42), and assay reagents for reduced

glutathione (GSH), superoxide dismutase (SOD), and catalase (CAT) were obtained from appropriate commercial sources. Cell-culture reagents were of cell-culture grade, while solvents used for chromatographic analysis were of HPLC grade.

2.3 Preparation of Hydroalcoholic Extract of *Celastrus paniculatus* Seeds

The coarsely powdered seeds were extracted using a hydroalcoholic solvent consisting of ethanol and purified water in a ratio of 70:30 (v/v). The powdered material was completely immersed in the extraction solvent and extracted under controlled conditions with intermittent agitation to facilitate the transfer of soluble phytoconstituents into the solvent phase. Following extraction, the liquid extract was separated by filtration, and the residual plant material was re-extracted to maximize recovery of extractable constituents. The combined filtrates were concentrated under reduced pressure at a temperature not exceeding 40–45°C using a rotary vacuum evaporator. The concentrated extract was subsequently dried to obtain the hydroalcoholic extract of *C. paniculatus* seeds (CPHE). The dried extract was weighed, transferred to an airtight amber container, and stored under refrigerated conditions until further analysis. The percentage extraction yield was calculated as (Chahuan et al., 2023; Chintha & Wudayagiri, 2022; John et al., 2022; Thongon et al., 2026):

Extraction yield (%) = (Weight of dried extract / Weight of powdered seed material used for extraction) × 100

2.4 Preliminary Phytochemical Screening

CPHE was subjected to qualitative phytochemical screening using established chemical tests to determine the major classes of secondary metabolites present in the extract. Tests were performed for alkaloids, phenolic compounds, flavonoids, tannins, terpenoids/triterpenoids, steroids, saponins, and glycosides. Appropriate reagent blanks were included where necessary. The results were recorded qualitatively according to the presence or absence of characteristic colour development or precipitation (Harborne, 1998; Harborne, 2012).

2.5 Determination of Total Phenolic Content

The total phenolic content (TPC) of CPHE was determined using the Folin–Ciocalteu colorimetric method. An appropriately diluted solution of CPHE was mixed with Folin–Ciocalteu reagent, followed by sodium carbonate solution. The reaction mixture was incubated under protected conditions for adequate colour development, and absorbance was measured spectrophotometrically at approximately 760–765 nm. A calibration curve was prepared using gallic acid at different concentrations. TPC was calculated from the regression equation of the gallic acid calibration curve and expressed as milligrams of gallic acid equivalents per gram of dried extract (mg GAE/g extract). Measurements were performed in triplicate (Harborne, 1998; Harborne, 2012).

2.6 Determination of Total Flavonoid Content

The total flavonoid content (TFC) of CPHE was determined using the aluminium chloride colorimetric method. An appropriately diluted extract solution was allowed to react with aluminium chloride under controlled conditions. Following incubation, absorbance was measured spectrophotometrically at the wavelength appropriate for the aluminium–flavonoid complex. Quercetin was used to construct the calibration curve. TFC was calculated from the corresponding regression equation and expressed as milligrams of quercetin equivalents per gram of dried extract (mg QE/g extract). All measurements were carried out in triplicate (Harborne, 1998; Harborne, 2012).

2.7 Chromatographic Standardization of CPHE

Chromatographic profiling of CPHE was performed using high-performance liquid chromatography coupled with photodiode-

array detection (HPLC-PDA). A known quantity of the dried extract was dissolved in a suitable HPLC-grade solvent, sonicated to ensure complete extraction of soluble constituents, and filtered through a 0.45 µm membrane filter before injection. Chromatographic separation was performed using a reversed-phase C18 analytical column. A suitable aqueous phase and organic modifier were employed as the mobile-phase system under gradient conditions to obtain adequate separation of the major extract constituents. The chromatogram was recorded over a suitable UV spectral range using the PDA detector. The chemical fingerprint was characterized according to the number, retention times, relative intensities, and UV absorption characteristics of the major chromatographic peaks. Where an authenticated reference standard was available, the corresponding marker constituent was identified by comparison of its retention time and UV spectrum with those of the reference standard and quantified using an external calibration curve. The chromatographic profile was used as a chemical standardization parameter for the CPHE batch employed throughout the biological experiments (Harborne, 1998; Harborne, 2012).

2.8 DPPH Radical-Scavenging Assay

The free-radical-scavenging activity of CPHE was determined using the DPPH assay. Different concentrations of CPHE were mixed with freshly prepared DPPH solution and incubated in the dark at room temperature. After completion of the reaction period, absorbance was measured at approximately 517 nm against an appropriate blank. A suitable standard antioxidant was included as the positive control. DPPH radical-scavenging activity was calculated as (Adel-Mehraban et al., 2024; Ncube et al., 2021; Parfait et al., 2022; Stefanis et al., 2023):

$$\text{DPPH scavenging activity (\%)} = [(A_{control} - A_{sample}) / A_{control}] \times 100$$

where Acontrol represents the absorbance of the DPPH solution without extract and Asample represents the absorbance in the presence of CPHE. A concentration-response curve was constructed, and the concentration required to produce 50% radical scavenging (IC50) was determined by nonlinear regression. Experiments were conducted in triplicate.

2.9 ABTS Radical-Scavenging Assay

The antioxidant activity of CPHE was additionally evaluated using the ABTS radical-cation decolorization assay. ABTS radical cations (ABTS•+) were generated by reacting ABTS with potassium persulfate and allowing the mixture to stand in the dark until radical formation was complete. Before analysis, the radical solution was diluted to an appropriate initial absorbance.

Different concentrations of CPHE were mixed with the ABTS•+ working solution and incubated for the specified reaction period. Absorbance was subsequently recorded at approximately 734 nm. A standard antioxidant was analyzed under identical conditions. ABTS radical-scavenging activity was calculated as (Adel-Mehraban et al., 2024; Ncube et al., 2021; Parfait et al., 2022; Stefanis et al., 2023):

$$\text{ABTS scavenging activity (\%)} = [(A_{control} - A_{sample}) / A_{control}] \times 100$$

The IC50 value was obtained from the concentration-response curve. All experiments were performed in triplicate.

2.10 In Vitro Acetylcholinesterase Inhibitory Activity

The acetylcholinesterase (AChE)-inhibitory activity of CPHE was evaluated using Ellman's colorimetric method with acetylthiocholine iodide as the enzyme substrate. The reaction mixture contained AChE, phosphate buffer, DTNB, and different concentrations of CPHE. Following a suitable pre-incubation period, the enzymatic reaction was initiated by addition of acetylthiocholine iodide. Hydrolysis of acetylthiocholine produces thiocholine, which reacts with DTNB to form a yellow-coloured product. The change in absorbance was monitored at

approximately 412 nm using a microplate reader or UV-visible spectrophotometer. Donepezil was included as the positive AChE-inhibitory control. AChE inhibition was calculated relative to the enzyme control after appropriate correction for sample and reagent blanks (Flores-Melivilu et al., 2026; Lee et al., 2025; Schwarthoff et al., 2021; Zhao et al., 2026):

AChE inhibition (%) = [(Acontrol − Asample) / Acontrol] × 100

Concentration-response curves were generated for CPHE and the reference inhibitor, and IC50 values were calculated by nonlinear regression. Experiments were conducted in triplicate.

2.11 SH-SY5Y Cell Culture

Human SH-SY5Y neuroblastoma cells were used for the cell-based neuroprotection experiments. Cells were maintained in DMEM/F-12 medium supplemented with 10% FBS and 1% penicillin-streptomycin solution. Cultures were maintained at 37°C in a humidified incubator containing 5% CO2. Cells were subcultured at appropriate confluence using trypsin-EDTA and were used within a controlled passage range to minimize phenotypic variation between experiments. Cell morphology and growth characteristics were routinely examined using an inverted microscope (Gardón et al., 2022; Palanivel et al., 2022; Tan et al., 2026).

2.12 Neuronal Differentiation of SH-SY5Y Cells

Before neuroprotection experiments, SH-SY5Y cells were differentiated toward a neuronal phenotype using all-trans-retinoic acid. Cells were seeded at an appropriate density and allowed to adhere before exposure to differentiation medium containing retinoic acid. The differentiation medium was renewed at predetermined intervals, and differentiation was continued until characteristic neuronal morphological changes, including reduced proliferation and neurite extension, were evident. Differentiated cells were subsequently used for cytocompatibility, amyloid-β-induced injury, intracellular ROS, cellular AChE, and antioxidant-defence studies (Gardón et al., 2022; Palanivel et al., 2022; Tan et al., 2026).

2.13 Cytocompatibility and Selection of CPHE Concentrations

The effect of CPHE alone on neuronal cell viability was initially evaluated to identify concentrations suitable for the subsequent neuroprotection experiments. Differentiated SH-SY5Y cells were seeded into 96-well plates and allowed to stabilize. Cells were then exposed to increasing concentrations of CPHE, initially covering a concentration range of 5–200 µg/mL, for a defined exposure period. Cell viability was determined using the MTT assay. After treatment, MTT solution was added to each well and the cells were incubated to permit viable cellular oxidoreductases to convert MTT to insoluble formazan. The medium was subsequently removed, the formazan crystals were dissolved in DMSO, and absorbance was measured at approximately 570 nm. Cell viability was calculated as (Fotakis & Timbrell, 2006; Gardón et al., 2022; Palanivel et al., 2022; Tan et al., 2026; van Meerloo et al., 2011):

Cell viability (%) = (Absorbance of treated cells / Absorbance of untreated control cells) × 100

Three concentrations demonstrating acceptable cytocompatibility were selected as low, medium, and high CPHE concentrations for subsequent experiments.

2.14 Preparation of Amyloid-β1–42 and Induction of Neuronal Injury

Synthetic Aβ1-42 peptide was used to establish amyloid-associated neuronal injury. The peptide was initially dissolved according to the manufacturer's recommended procedure and subjected to controlled pre-incubation to generate the required amyloid preparation. Aliquots were prepared where appropriate to minimize repeated freeze-thaw cycles. A preliminary concentration-response experiment was conducted to identify an Aβ1-42 exposure condition capable of producing reproducible, moderate neuronal injury while retaining a sufficient viable-

cell population for detection of neuroprotective effects. The selected Aβ1-42 concentration and exposure period were subsequently maintained throughout the definitive experiments (Arrazola Sastre et al., 2023; Flores-Melivilu et al., 2026; Hacımüftüoğlu et al., 2026; Toyokawa et al., 2026; Zedde et al., 2025).

2.15 Experimental Design for the Neuroprotection Study

Differentiated SH-SY5Y cells were allocated to the following experimental groups (Arrazola Sastre et al., 2023; Toyokawa et al., 2026):

Group	Treatment
Normal control	Untreated cells
Aβ control	Cells exposed to Aβ1-42
Positive control	Aβ1-42 + reference treatment
CPHE-L	Aβ1-42 + low concentration of CPHE
CPHE-M	Aβ1-42 + medium concentration of CPHE
CPHE-H	Aβ1-42 + high concentration of CPHE

The low, medium, and high CPHE concentrations were selected from the preceding cytocompatibility study. The reference treatment was selected on the basis of the endpoint being investigated and its suitability for the Aβ1–42 neuronal-injury model. The same treatment paradigm was maintained across the principal cell-based assays to permit direct comparison of cell viability, intracellular ROS, antioxidant defences, and cellular AChE activity.

2.16 Evaluation of Neuroprotective Activity by MTT Assay

The neuroprotective effect of CPHE against Aβ1–42-induced cellular injury was evaluated using the MTT assay. Differentiated SH-SY5Y cells were exposed to the selected CPHE concentrations and Aβ1–42 according to the predetermined treatment protocol. Following completion of the treatment period, cellular viability was determined as described above. Viability of untreated control cells was considered 100%. The extent of Aβ1–42-induced reduction in viability and the ability of CPHE to prevent or attenuate this reduction were compared among the experimental groups (Arrazola Sastre et al., 2023; Fotakis & Timbrell, 2006; Morgan, 1998; Toyokawa et al., 2026).

2.17 Measurement of Intracellular Reactive Oxygen Species

Intracellular reactive oxygen species (ROS) generation was determined using the DCFH-DA fluorescence assay. Following the experimental treatments, cells were washed with PBS and incubated with DCFH-DA under light-protected conditions. Intracellular esterases convert DCFH-DA to non-fluorescent DCFH, which is oxidized by reactive species to fluorescent dichlorofluorescein. After incubation, excess probe was removed by washing. Fluorescence was quantified using a fluorescence microplate reader at appropriate excitation and emission wavelengths. Representative fluorescence micrographs were additionally acquired under identical imaging conditions to permit qualitative visualization of intracellular ROS generation.

ROS levels were expressed relative to the untreated control. Comparisons were made between the normal control, Aβ1–42 injury control, positive control, and CPHE-treated groups (Fotakis & Timbrell, 2006; Morgan, 1998).

2.18 Determination of Cellular Acetylcholinesterase Activity

Following the respective treatments, cells were harvested and lysed under cold conditions. Cellular lysates were clarified by centrifugation, and the resulting supernatants were used for measurement of AChE activity using the Ellman reaction. Acetylthiocholine iodide was used as the substrate and DTNB as the chromogenic reagent. Enzymatic activity was determined from the rate of colour development at approximately 412 nm. Where required, AChE activity was normalized to the protein content of the corresponding cell

lysate. The results were expressed relative to the untreated control or as specific enzyme activity, depending on the analytical method used (Faldu et al., 2023; Lee et al., 2025; Parfait et al., 2022).

2.19 Determination of Reduced Glutathione

Intracellular reduced glutathione was determined in cell lysates using a DTNB-based colorimetric assay or a validated commercial assay kit. Following treatment, cells were harvested, lysed, and processed to obtain clarified samples. The reaction of sulfhydryl groups in reduced glutathione with DTNB produces a yellow-coloured chromophore, which was quantified spectrophotometrically. GSH concentration was calculated using an appropriate standard calibration curve and normalized to cellular protein content where applicable (Duperray et al., 2022; Ivanov et al., 2022; Wang et al., 2025; Ye et al., 2022).

2.20 Determination of Superoxide Dismutase Activity

Superoxide dismutase activity was determined in cell lysates using a validated spectrophotometric method or commercial SOD assay kit. The assay was based on the ability of SOD to inhibit a superoxide-dependent chromogenic reaction. Samples were processed according to the validated assay procedure, and absorbance was measured at the specified wavelength. SOD activity was calculated according to the assay principle and expressed as units per milligram of cellular protein or relative activity compared with the untreated control (Kuthoor et al., 2022; Pavlenko et al., 2025; Ri et al., 2022).

2.21 Determination of Catalase Activity

Catalase activity was determined in treated-cell lysates using a validated spectrophotometric assay. The assay was based on the decomposition of hydrogen peroxide by catalase. Enzymatic activity was determined from the rate of hydrogen peroxide decomposition or the corresponding chromogenic reaction, depending on the assay system employed. Catalase activity was normalized to cellular protein content and compared among the experimental groups (Aslantas et al., 2022; Montejo et al., 2026; Tolmacheva et al., 2024).

2.22 Determination of Cellular Protein Content

Total protein content of the cellular lysates was determined using an appropriate validated protein assay with bovine serum albumin as the calibration standard. Protein concentrations were used to normalize cellular AChE, SOD, CAT, and GSH measurements where required, thereby minimizing differences arising from variation in cellular biomass between experimental groups (Aslantas et al., 2022; Montejo et al., 2026; Tolmacheva et al., 2024).

2.23 Statistical Analysis

All cell-free experiments were performed in at least three independent determinations. Cell-based experiments were conducted as a minimum of three independent biological experiments, with appropriate technical replicates within each experiment. Results were expressed as mean ± standard deviation (SD). Concentration-response data from the DPPH, ABTS, and AChE-inhibition assays were analyzed by nonlinear regression, and IC50 values were reported with 95% confidence intervals where appropriate. For comparisons involving more than two experimental groups, data were analyzed using one-way analysis of variance (ANOVA), followed by Tukey's multiple-comparison test when the overall ANOVA indicated statistical significance. Assumptions of normality and homogeneity of variance were assessed before application of parametric tests. Where these assumptions were not satisfied, an appropriate non-parametric alternative was employed. A value of $p < 0.05$ was considered statistically significant. Statistical analysis and graphical presentation were performed using appropriate validated statistical software.

3. Results and Discussion

3.1 Extraction and Phytochemical Characteristics of CPHE

Hydroalcoholic extraction of 250 g of powdered *Celastrus paniculatus* seeds yielded 31.85 g of dried extract, corresponding to an extraction yield of 12.74% w/w. The 70% ethanol–water system was selected to provide a relatively broad extraction range encompassing polar and moderately non-polar phytoconstituents. The resulting hydroalcoholic extract of *C. paniculatus* seeds (CPHE) was used throughout the phytochemical, biochemical, and cell-based investigations. Preliminary phytochemical screening demonstrated the presence of alkaloids, phenolic compounds, flavonoids, tannins, terpenoids/triterpenoids, steroids, saponins, and glycosides. Since qualitative colour and precipitation reactions are presumptive rather than compound-specific, these findings were used only to characterize broad phytochemical classes and were complemented by quantitative and chromatographic analyses.

Table 1. Extraction characteristics and phytochemical profile of hydroalcoholic extract of *Celastrus paniculatus* seeds

Parameter	Result
Seed powder used	250 g
Dried extract obtained	31.85 g
Extraction yield	12.74% w/w
Total phenolic content	68.42 ± 2.31 mg GAE/g
Total flavonoid content	31.76 ± 1.48 mg QE/g
Alkaloids	+
Phenolic compounds	+
Flavonoids	+
Tannins	+
Terpenoids/triterpenoids	+
Steroids	+
Saponins	+
Glycosides	+

Values for total phenolic and flavonoid contents represent mean ± SD (n = 3). + indicates a positive qualitative phytochemical reaction.

Quantitative analysis showed a total phenolic content of 68.42 ± 2.31 mg GAE/g extract and a total flavonoid content of 31.76 ± 1.48 mg QE/g extract. These findings demonstrate that CPHE contains an appreciable fraction of compounds capable of participating in redox reactions. Phenolic hydroxyl groups can contribute to radical-quenching activity through electron or hydrogen donation, although TPC and TFC assays are nonspecific and cannot identify the compounds responsible for biological activity. Therefore, the observed values were interpreted as batch-standardization parameters rather than direct evidence of neuroprotective efficacy.

3.2 Chromatographic Fingerprinting of CPHE

HPLC-PDA analysis produced a reproducible multicomponent chromatographic fingerprint. Seven major peaks were observed, together accounting for 81.78% of the integrated chromatographic area. The most prominent peak occurred at a retention time of 13.72 min and represented 18.56% of the total peak area, followed by peaks at 7.86 min (14.62%), 17.45 min (12.38%), and 21.18 min (10.74%).

Table 2. Major peaks observed in the HPLC-PDA fingerprint of CPHE

Peak	Retention time (min)	Relative peak area (%)
P1	3.21	6.84
P2	5.47	9.73
P3	7.86	14.62
P4	10.34	8.91
P5	13.72	18.56
P6	17.45	12.38
P7	21.18	10.74
Other minor peaks	—	18.22

The chromatographic profile confirms the chemically heterogeneous nature of CPHE and provides a practical fingerprint for the

experimental batch. Importantly, individual peaks were not assigned to specific phytochemicals solely on the basis of retention time. Definitive identification would require comparison with authenticated standards and/or appropriate structural characterization. This conservative interpretation is particularly important for botanical extracts because retention-time similarity alone does not establish molecular identity.

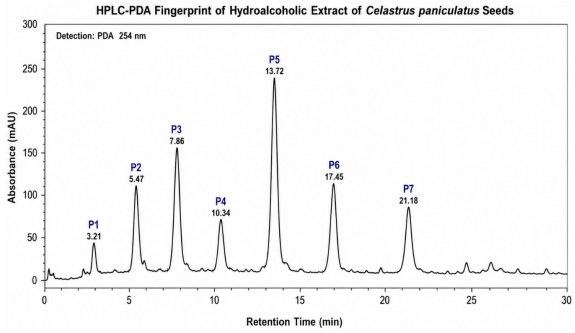


Figure 1. Representative HPLC-PDA fingerprint of the hydroalcoholic extract of *Celastrus paniculatus* seeds showing the major chromatographic peaks used for batch characterization.

Together, extraction yield, TPC, TFC, and the HPLC fingerprint establish a more meaningful standardization framework than qualitative phytochemical screening alone and provide reference parameters against which subsequent CPHE batches can be compared.

3.3 Free-Radical-Scavenging Activity of CPHE

CPHE demonstrated concentration-dependent activity in both DPPH and ABTS radical-scavenging assays. DPPH inhibition increased from 14.8 ± 1.2% at 10 µg/mL to 84.7 ± 1.6% at 200 µg/mL, while ABTS inhibition increased from 18.6 ± 1.3% to 88.3 ± 1.5% over the same concentration range.

Table 3. Antioxidant and acetylcholinesterase-inhibitory activities of CPHE

CPHE concentration (µg/mL)	DPPH inhibition (%)	ABTS inhibition (%)	AChE inhibition (%)
10	14.8 ± 1.2	18.6 ± 1.3	11.7 ± 1.1
25	27.9 ± 1.5	32.4 ± 1.5	22.9 ± 1.4
50	43.8 ± 1.7	49.7 ± 1.8	39.8 ± 1.6
100	66.5 ± 2.0	71.8 ± 1.9	61.7 ± 1.9
200	84.7 ± 1.6	88.3 ± 1.5	80.6 ± 1.7
IC50 (µg/mL)	**61.8**	**50.7**	**~70**

Values represent mean ± SD (n = 3). IC50 values were derived from concentration-response analysis.

The estimated IC50 values were 61.8 µg/mL for DPPH and 50.7 µg/mL for ABTS. The somewhat lower ABTS IC50 indicates greater apparent activity under the ABTS assay conditions. Differences between the two assays are expected because DPPH and ABTS differ in radical chemistry, solvent compatibility, and accessibility to antioxidant molecules. The antioxidant activity is compatible with the measured phenolic and flavonoid contents of CPHE. Nevertheless, these chemical assays do not reproduce intracellular oxidative processes and therefore should not independently be described as evidence of neuronal protection. Their importance in the present study lies in establishing intrinsic radical-scavenging capacity that can subsequently be compared with the cellular ROS and endogenous antioxidant-defense results.

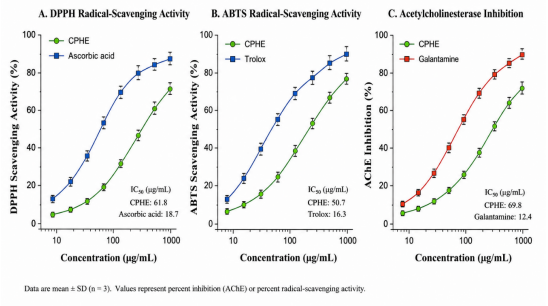


Figure 2. Concentration-response profiles of CPHE for DPPH and ABTS radical-scavenging activity and acetylcholinesterase inhibition.

3.4 Acetylcholinesterase-Inhibitory Activity

CPHE also inhibited AChE in a concentration-dependent manner. Inhibition increased from 11.7 ± 1.1% at 10 µg/mL to 80.6 ± 1.7% at 200 µg/mL, with an estimated IC50 of approximately 70 µg/mL. This observation is pharmacologically relevant because excessive hydrolysis of acetylcholine by cholinesterases contributes to impaired cholinergic neurotransmission, and inhibition of AChE remains an established symptomatic therapeutic strategy in Alzheimer's disease. The result therefore provides a functional basis for investigating whether CPHE can influence AChE activity under neuronal stress conditions. However, the activity of the crude extract should not be interpreted as equivalent to that of a purified clinical AChE inhibitor. CPHE represents a chemically complex mixture, and its mass-based IC50 cannot be directly equated with the potency of donepezil without accounting for differences in molecular composition and concentration units. The importance of the result is instead the demonstration of reproducible concentration-dependent AChE inhibition.

3.5 Cytocompatibility and Selection of CPHE Concentrations

Determination of extract cytocompatibility was necessary before assessment of neuroprotection. CPHE concentrations between 5 and 50 µg/mL produced little change in SH-SY5Y viability, whereas viability remained 91.8 ± 2.6% at 100 µg/mL. Increasing the concentration to 200 µg/mL reduced viability to 78.6 ± 3.0%.

Table 4. Cytocompatibility of CPHE and optimization of Aβ1-42-induced neuronal injury

CPHE (µg/mL)	Cell viability (%)	Aβ1-42 (µM)	Cell viability (%)
Control	100.0 ± 2.1	Control	100.0 ± 2.3
5	101.2 ± 2.0	2.5	90.7 ± 2.5
10	100.4 ± 2.2	5	80.9 ± 2.8
25	98.7 ± 2.1	10	65.8 ± 2.7
50	96.5 ± 2.4	20	50.9 ± 2.9
100	91.8 ± 2.6	—	—
200	78.6 ± 3.0	—	—

Values represent mean ± SD from independent experiments.

On this basis, 25, 50, and 100 µg/mL were selected as the low, medium, and high concentrations for neuroprotection studies. The 200 µg/mL concentration was excluded because the reduction in viability could confound interpretation of subsequent protective effects. Aβ1-42 produced a concentration-dependent decrease in cell viability. Viability declined from 90.7 ± 2.5% at 2.5 µM to 50.9 ± 2.9% at 20 µM. A concentration of 10 µM, which reduced viability to 65.8 ± 2.7%, was selected for the definitive experiments. This intermediate degree of injury provided sufficient dynamic range to detect protective effects without inducing near-maximal cytotoxicity.

3.6 CPHE Protects SH-SY5Y Cells Against Aβ1–42-Induced Injury

Exposure to 10 µM Aβ1-42 markedly reduced SH-SY5Y cell viability from 100.0 ± 2.2% in untreated cells to 65.6 ± 2.8% ($p < 0.001$), confirming substantial amyloid-associated neuronal injury. Treatment with CPHE produced concentration-dependent protection. Viability increased to 73.8 ± 2.6%, 82.1 ± 2.5%, and 90.4 ± 2.3% at 25, 50, and 100 µg/mL, respectively. The effect at 25 µg/mL was significant relative to the Aβ control ($p < 0.05$), while the 50 and 100 µg/mL treatments produced stronger protection ($p < 0.001$).

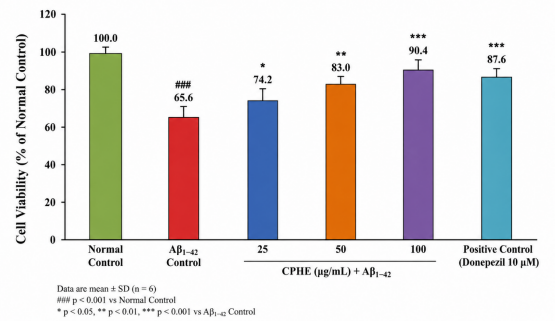


Figure 3. Effect of CPHE on viability of differentiated SH-SY5Y cells exposed to Aβ1–42. Values are expressed as mean ± SD.

The highest CPHE concentration restored viability close to the untreated-cell level but did not artificially increase it above baseline. This finding is important because the cytocompatibility experiment independently demonstrated that 100 µg/mL CPHE was reasonably well tolerated in the absence of Aβ1–42. Thus, the increased viability under amyloid challenge is consistent with a protective response rather than nonspecific stimulation of the MTT signal. The positive-control group showed 88.9 ± 2.4% viability, providing an assay benchmark and confirming that the Aβ-induced injury remained pharmacologically modifiable.

3.7 Attenuation of Aβ1–42-Induced Intracellular ROS Generation

The neuroprotective response was accompanied by marked changes in intracellular oxidative stress. Aβ1–42 increased relative DCF fluorescence to 224.6 ± 8.7% of the untreated control, indicating more than a twofold increase in probe oxidation. CPHE progressively reduced the signal to 188.7 ± 7.6%, 151.8 ± 6.5%, and 119.7 ± 5.4% at 25, 50, and 100 µg/mL, respectively.

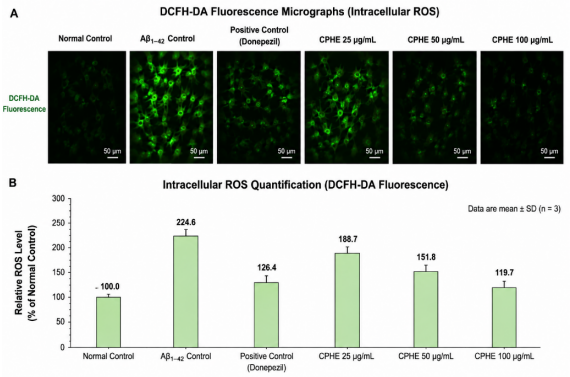


Figure 4. Representative DCFH-DA fluorescence micrographs and quantitative analysis of intracellular ROS generation in untreated, Aβ1–42-treated, positive-control, and CPHE-treated SH-SY5Y cells.

The ROS findings provide a cellular correlate to the DPPH and ABTS results. Unlike the cell-free radical assays, DCFH-DA measurements demonstrate that CPHE attenuated oxidative conditions within Aβ-challenged neuronal cells. The agreement between chemical antioxidant activity and intracellular ROS attenuation strengthens the evidence for an antioxidant contribution to neuroprotection. Nevertheless, DCFH-DA is a general oxidation-sensitive probe and does not identify individual reactive oxygen species. Accordingly, the results are interpreted as changes in overall intracellular oxidative activity rather than evidence for selective scavenging of a particular ROS species.

3.8 Effect of CPHE on Cellular AChE Activity

Aβ1–42 exposure increased cellular AChE activity to 151.7 ± 5.6% relative to the untreated control. CPHE reduced this increase in a concentration-dependent manner, with relative activities of 137.9 ± 5.1%, 120.8 ± 4.7%, and 108.9 ± 4.3% at 25, 50, and 100 µg/mL, respectively. The positive-control group showed an activity of 106.8 ± 4.2%.

Table 5. Effects of CPHE on intracellular ROS, AChE activity, and antioxidant defenses in Aβ1–42-injured SH-SY5Y cells

Group	ROS (%)	AChE activity (%)	SOD (%)	CAT (%)	GSH (%)
Normal control	100.0 ± 4.2	100.0 ± 3.8	100.0 ± 4.1	100.0 ± 3.9	100.0 ± 4.0
Aβ1–42 control	224.6 ± 8.7	151.7 ± 5.6	52.8 ± 3.5	48.7 ± 3.2	45.6 ± 3.1
Positive control	126.4 ± 5.9	106.8 ± 4.2	89.7 ± 3.8	87.4 ± 3.7	90.2 ± 3.6
CPHE 25 µg/mL	188.7 ± 7.6	137.9 ± 5.1	63.9 ± 3.6	60.8 ± 3.4	59.7 ± 3.5
CPHE 50 µg/mL	151.8 ± 6.5	120.8 ± 4.7	77.8 ± 3.9	74.6 ± 3.6	75.9 ± 3.8
CPHE 100 µg/mL	119.7 ± 5.4	108.9 ± 4.3	91.2 ± 4.0	88.9 ± 3.8	89.7 ± 3.9

Values are expressed relative to the untreated control and represent mean ± SD.

The cellular findings are consistent with the direct AChE-inhibition assay, in which CPHE produced concentration-dependent enzyme inhibition. Together, these results support cholinesterase modulation as one component of the biological activity of CPHE.

3.9 Restoration of Cellular Antioxidant Defenses

Aβ1–42-induced oxidative injury was associated not only with increased intracellular ROS but also with substantial impairment of endogenous antioxidant defences. Relative SOD activity decreased to 52.8 ± 3.5%, catalase activity to 48.7 ± 3.2%, and GSH level to 45.6 ± 3.1% of normal-control values. CPHE produced a concentration-dependent recovery of all three parameters. At 25 µg/mL, SOD, CAT, and GSH increased to 63.9 ± 3.6%, 60.8 ± 3.4%, and 59.7 ± 3.5%, respectively. At 50 µg/mL, corresponding values increased further to 77.8 ± 3.9%, 74.6 ± 3.6%, and 75.9 ± 3.8%. The highest concentration, 100 µg/mL, restored SOD to 91.2 ± 4.0%, CAT to 88.9 ± 3.8%, and GSH to 89.7 ± 3.9%, approaching the values observed with the positive control.

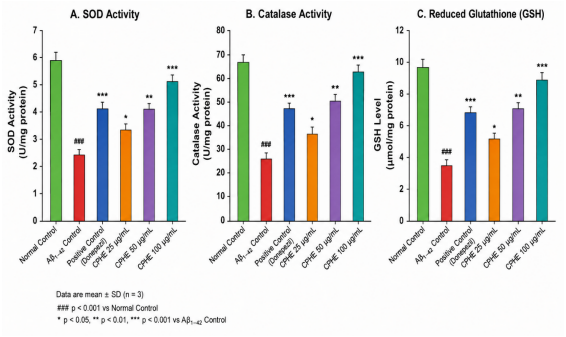


Figure 5. Effects of CPHE on SOD activity, catalase activity, and reduced glutathione levels in Aβ1–42-injured differentiated SH-SY5Y cells.

The simultaneous reduction in ROS and recovery of SOD, CAT, and GSH provides stronger evidence for attenuation of cellular oxidative stress than either type of measurement alone. SOD contributes to the conversion of superoxide radicals to hydrogen peroxide, catalase participates in hydrogen peroxide decomposition, and GSH represents a major intracellular redox buffer. Their depletion following Aβ exposure is therefore compatible with disruption of cellular redox homeostasis. CPHE substantially attenuated these disturbances, particularly at 50 and 100 µg/mL. The findings suggest that its protective activity may involve both direct radical-scavenging properties and preservation of endogenous antioxidant capacity.

3.10 Integrated Interpretation of Neuroprotective Activity

Taken together, the findings demonstrate a coherent relationship between the phytochemical characteristics and biological effects of CPHE. The extract contained measurable phenolic and flavonoid fractions and displayed concentration-dependent activity in two

chemically distinct radical-scavenging systems. CPHE additionally inhibited AChE in the cell-free assay, establishing a second functional activity relevant to cholinergic dysfunction. More importantly, these properties translated into measurable effects in differentiated neuronal cells. Aβ1-42 exposure caused a coordinated pattern of cellular disturbance characterized by reduced viability, increased intracellular ROS, increased AChE activity, and depletion of SOD, catalase, and GSH. CPHE opposed each of these alterations in a concentration-dependent manner. At 100 µg/mL, cell viability recovered from 65.6% to 90.4%, ROS decreased from 224.6% to 119.7%, and cellular AChE activity decreased from 151.7% to 108.9% relative to normal-control levels. Antioxidant-defence parameters were simultaneously restored to approximately 89–91% of control values.

4. Conclusion

The present study demonstrated the in vitro neuroprotective potential of a phytochemically standardized hydroalcoholic extract of *Celastrus paniculatus* seeds (CPHE) against amyloid-β1–42-induced neuronal injury. Phytochemical characterization revealed the presence of multiple secondary-metabolite classes, with measurable phenolic and flavonoid contents, while HPLC-PDA analysis provided a reproducible chromatographic fingerprint for chemical standardization of the experimental extract. CPHE exhibited concentration-dependent DPPH and ABTS radical-scavenging activities together with acetylcholinesterase-inhibitory activity. More importantly, these biochemical properties were accompanied by significant protection of differentiated SH-SY5Y cells against Aβ1–42-induced injury. CPHE improved cellular viability, markedly reduced intracellular ROS generation, attenuated the Aβ-associated increase in cellular AChE activity, and restored SOD, catalase, and reduced glutathione levels toward normal-control values. The greatest protective response was observed at 100 µg/mL, indicating a clear concentration-dependent effect within the cytocompatible concentration range. Collectively, the findings suggest that the neuroprotective activity of CPHE is associated with complementary antioxidant and cholinesterase-modulating effects. The study does not establish involvement of a specific intracellular signalling pathway or demonstrate therapeutic efficacy in Alzheimer's disease; rather, it provides mechanistically relevant in vitro evidence supporting further investigation of *C. paniculatus* seeds as a source of neuroprotective phytoconstituents. Future studies should identify the constituents responsible for these activities and establish their contribution to the observed effects using more advanced disease-relevant experimental systems.

References

Adel-Mehraban, M. S., Tabatabaei-Malazy, O., Manayi, A., Alatab, S., Mohseni, S., Fana, S. E., Asili, P., Bahramsoltani, R., Esmaeili, F., & Azizi, B. (2024). Antioxidative and Anti-inflammatory Effects of Plant-derived Hypoglycemic Medicines: An In vivo/In vitro Systematic Review. *Curr Top Med Chem*, *24*(16), 1408-1450. https://doi.org/10.2174/0115680266295032240415064750

Aleem, M. (2023). Phytochemistry and pharmacology of Celastrus paniculatus Wild.: a nootropic drug. *J Complement Integr Med*, *20*(1), 24-46. https://doi.org/10.1515/jcim-2021-0251

Arrazola Sastre, A., Luque Montoro, M., Llavero, F., & Zugaza, J. L. (2023). Amyloid β(1-42) Oligomers Induce Galectin-1(S8) O-GlcNAcylation Leading to Microglia Migration. *Cells*, *12*(14). https://doi.org/10.3390/cells12141876

Asken, B. M., Brett, B. L., Barr, W. B., Banks, S., Wethe, J. V., Dams-O'Connor, K., Stern, R. A., & Alosco, M. L. (2025). Chronic traumatic encephalopathy: State-of-the-science update and narrative review. *Clin Neuropsychol*, *39*(8), 2159-2183. https://doi.org/10.1080/13854046.2025.2454047

Aslantas, E. E., Buzoglu, H. D., Muftuoglu, S. F., Atilla, P., Karapinar, S. P., & Aksoy, Y. (2022). Effects of aging and inflammation on catalase activity in human dental pulp. *Arch Oral Biol*, *141*, 105482. https://doi.org/10.1016/j.archoralbio.2022.105482

Bayraktaroglu, I., Ortí-Casañ, N., Van Dam, D., De Deyn, P. P., & Eisel, U. L. M. (2025). Systemic inflammation as a central player in the initiation and development of Alzheimer's disease. *Immun Ageing*, *22*(1), 33. https://doi.org/10.1186/s12979-025-00529-5

Chahuan, S., Grover, S., & Singh, S. (2023). Amelioration of modified chronic unpredictable stress using Celastrus paniculatus seed oil alone and in combination with fluoxetine. *Drug Chem Toxicol*, *46*(5), 879-894. https://doi.org/10.1080/01480545.2022.2105862

Chintha, V., & Wudayagiri, R. (2022). Isolation and neuroprotective prospective of novel bioactive compound "3-(3,4-dimethoxyphenyl)-1-(4-methoxyphenyl) prop-2-en-1-one" against ketamine-induced cognitive deficits in schizophrenia: an experimental study. *Nat Prod Res*, *36*(5), 1352-1358. https://doi.org/10.1080/14786419.2020.1869968

Duperray, J., Sergheraert, R., Chalothorn, K., Tachalerdmanee, P., & Perin, F. (2022). The effects of the oral supplementation of L-Cystine associated with reduced L-Glutathione-GSH on human skin pigmentation: a randomized, double-blinded, benchmark- and placebo-controlled clinical trial. *J Cosmet Dermatol*, *21*(2), 802-813. https://doi.org/10.1111/jocd.14137

Dwivedi, S., Barwant, M. M., Ali, U. M., & Tufa, A. (2026). Mycogenic synthesis of ZnO nanoparticles using an endophytic Aspergillus niger isolate from Celastrus paniculatus: evaluation of multifunctional bioactivity for agricultural and antimicrobial applications. *Discov Nano*, *21*(1). https://doi.org/10.1186/s11671-026-04670-y

Faldu, K. G., Patel, S. S., & Shah, J. S. (2023). Celastrus paniculatus oil ameliorates NF-KB mediated neuroinflammation and synaptic plasticity in the scopolamine-induced cognitive impairment rat model. *Metab Brain Dis*, *38*(4), 1405-1419. https://doi.org/10.1007/s11011-023-01186-7

Favari, E., & Parolini, C. (2025). Marine Bioactive Components and Chronic Neuroinflammation: Focus on Neurodegenerative Disease. *Mar Drugs*, *23*(11). https://doi.org/10.3390/md23110446

Flores-Melivilu, D., Carrazana, E., García, N., Alarcón, S., Caru-Ruiz, M., Chacón-Fuentes, M., Santos, N., Ahumada, M., Nova, E., Diaz-Espinoza, R., Sanhueza, M., Hormazábal, E., & Salvadores, N. (2026). Aristotelia chilensis Fruit Extracts Exhibit Neuroprotective Properties Against Alzheimer's Disease Related Mechanisms. *Mol Neurobiol*, *63*(1). https://doi.org/10.1007/s12035-026-05855-3

Fotakis, G., & Timbrell, J. A. (2006). In vitro cytotoxicity assays: Comparison of LDH, neutral red, MTT and protein assay in hepatoma cell lines following exposure to cadmium chloride. *Toxicology Letters*, *160*, 171-177.

Gardón, D. P., Cervantes-Llanos, M., Matamoros, B. P., Rodríguez, H. C., Tan, C. Y., Marín-Prida, J., Falcón-Cama, V., Pavón-Fuentes, N., Lemus, J. G., Ruiz, L. C. B., Argudin, T. D., Donato, G. M., Perera, Y., Yang, K., & Pentón-Rol, G. (2022). Positive effects of Phycocyanobilin on gene expression in glutamate-induced excitotoxicity in SH-SY5Y cells and animal models of multiple sclerosis and cerebral ischemia. *Heliyon*, *8*(6), e09769. https://doi.org/10.1016/j.heliyon.2022.e09769

Gupta J, Sharma B, Sorout R, Singh RG, Ittishree, Sharma MC. Ginger (Zingiber officinale) in traditional Chinese medicine: A comprehensive review of its anti-inflammatory properties and clinical applications. Pharmacol Res Mod Chin Med. 2025;14:100561.

Hacımüftüoğlu, A., Saraçoğlu, N., Saffour, S., Abad, N., Kesgun, Y., Zegheb, N., Gundeger, E., Yeşilyurt, F., Ataş, M. N., Bati-Ayaz, G., Altunlu, Ö., Çınar, B., Yörük, M. A., Okkay, U., Özkaraca, M., Ateş, O., Taghizadehghalehjoughi, A., Lafzi, F., & Türkez, H. (2026). Multi-Target Neuroprotective Compound Exhibits EAAT2-Modulating and Alzheimer's Pathology-Attenuating Effects in In Vitro and In Vivo Models. *ACS Chem Neurosci*, *17*(10), 1919-1944. https://doi.org/10.1021/acschemneuro.5c00873

Harborne, J. B. (1998). *Phytochemical Methods: A Guide to Modern Techniques of Plant Analysis*. Springer.

Harborne, J. B. (2012). *Phytochemical Methods: A Guide to Modern Techniques of Plant Analysis*. Springer Netherlands. https://books.google.co.in/books?id=BlMpBgAAQBAJ

Husain A, Alouffi S, Khanam A, Akasha R, Farooqui A, Ahmad S. Therapeutic Efficacy of Natural Product 'C-Phycocyanin' in Alleviating Streptozotocin-Induced Diabetes via the Inhibition of Glycation Reaction in Rats. Int J Mol Sci. 2022;23(22):14235.

Ivanov, A. V., Popov, M. A., Aleksandrin, V. V., Kozhevnikova, L. M., Moskovtsev, A. A., Kruglova, M. P., Vladimirovna, S. E., Aleksandrovich, S. V., & Kubatiev, A. A. (2022). Determination of glutathione in blood via capillary electrophoresis with pH-mediated stacking. *Electrophoresis*, *43*(18-19), 1859-1870. https://doi.org/10.1002/elps.202200119

John, E., Mishra, B., Tripathi, A. S., & Aleesha, R. (2022). Protective effect of Celastrus paniculatus on cognitive function in glutamate-induced brain-injured mice by reducing the intracellular influx of Ca(). *Int J Dev Neurosci*, *82*(4), 331-338. https://doi.org/10.1002/jdn.10182

Jain BN, Jain V, Shete A. Antipsychotic activity of aqueous ethanolic extract of Tinospora Cordifolia in amphetamine challenged mice model. J Adv Pharm Technol Res. 2010;1(1):30-33.

Katramadou, A., Bender, E. S., & Kanakis, D. (2026). From Traumatic Brain Injury to Alzheimer's Disease: Multilevel Biomechanical, Neurovascular, and Molecular Mechanisms with Emerging Therapeutic Directions. *Int J Mol Sci*, *27*(3). https://doi.org/10.3390/ijms27031570

Kumar, N., & Jaitak, V. (2026). Celastrus paniculatus Willd.: An Extensive Review of Phytochemistry, Traditional Uses, Pharmacological Potential, and Safety Profile. *Phytother Res*, *40*(6), 3416-3477. https://doi.org/10.1002/ptr.70325

Kuthoor, J. M., Sunil, E. A., Raghavan, S. E., & Purushothaman, B. P. (2022). A comparative investigation of the activity of superoxide dismutase in patients with leukoplakia and healthy controls. *Indian J Dent Res*, *33*(3), 287-291. https://doi.org/10.4103/ijdr.ijdr_1009_21

Kwon, O. Y., & Lee, S. H. (2025). Therapeutic Potential of Ishige okamurae Yendo as a Multi-Target Inhibitor Against Dementia Symptoms. *Life (Basel)*, *15*(11). https://doi.org/10.3390/life15111699

Lee, S. S., Ko, D. H., Lee, G. Y., Kim, S. Y., Han, S. Y., Park, J. Y., Park, M., Kim, H. M., Kim, Y. E., & Yoo, Y. C. (2025). Neuroprotective Effect of Mixed Mushroom Mycelia Extract on Neurotoxicity and Neuroinflammation via Regulation of ROS-Induced Oxidative Stress in PC12 and BV2 Cells. *Cells*, *14*(13). https://doi.org/10.3390/cells14130977

Mali, S. C., Dhaka, A., Sharma, S., & Trivedi, R. (2026). Antimicrobial and antioxidant activity of green synthesized copper nanoparticles. *Prep Biochem Biotechnol*, 1-9. https://doi.org/10.1080/10826068.2026.2661962

Manoharan, N., Jayamurali, D., Sridhar, A., & Govindarajulu, S. N. (2025). Neuroprotective capacity of Celastrus paniculatus on rotenone-induced parkinsonism in zebrafish model. *Mol Biol Rep*, *52*(1), 272. https://doi.org/10.1007/s11033-025-10384-8

Marques, B. L., & Campos, A. C. (2024). Cannabidiol and Alzheimer's disease. *Int Rev Neurobiol*, *177*, 121-134. https://doi.org/10.1016/bs.irn.2024.04.014

Montejo, U., Beldarrain, G., Olza, S., Alart, J. A., Chillida, M., García-Alonso, I., Alonso-Alconada, D., Alonso-Varona, A., & Herrero de la Parte, B. (2026). Microplate assay for the quantification of catalase activity in biological samples. *Methods*, *246*, 186-194. https://doi.org/10.1016/j.ymeth.2025.12.009

Morgan, D. M. L. (1998). Tetrazolium (MTT) is an assay for cellular viability and activity. *Methods in Molecular Biology*, *79*, 179-184.

Ncube, S. F., McGaw, L. J., Njoya, E. M., Ndagurwa, H. G. T., Mundy, P. J., & Sibanda, S. (2021). In vitro antioxidant activity of crude extracts of Harpagophytum zeyheri and their anti-inflammatory and cytotoxicity activity compared with diclofenac. *BMC Complement Med Ther*, *21*(1), 238. https://doi.org/10.1186/s12906-021-03407-x

Palanivel, V., Gupta, V., Mirshahvaladi, S. S. O., Sharma, S., Gupta, V., Chitranshi, N., Mirzaei, M., Graham, S. L., & Basavarajappa, D. (2022). Neuroprotective Effects of Neuropeptide Y on Human Neuroblastoma SH-SY5Y Cells in Glutamate Excitotoxicity and ER Stress Conditions. *Cells*, *11*(22). https://doi.org/10.3390/cells11223665

Parfait, B., Galba Jean, B., Roger, P., Hervé Hervé, N. A., Balbine, K. K., Guillaume, C. W., Simon Desire, G. N., Linda, D. K. J., Léa Blondelle, K. D., & Germain, S. T. (2022). Antioxidant and Anticholinesterase Properties of the Aqueous Extract of Balanites aegyptiaca L. Delile Fruit

Pulp on Monosodium Glutamate-Induced Excitotoxicity in Swiss Mice. *Evid Based Complement Alternat Med*, *2022*, 7576132. https://doi.org/10.1155/2022/7576132

Pavlenko, T. A., Chesnokova, N. B., Beznos, O. V., Shikareva, N. N., Nodel, M. R., Shevtsova, K. V., Panina, U. V., Shteinberg, D. A., Kukharskaya, O. A., Sukhanova, I. S., Pukaeva, N. E., Kukharsky, M. S., & Ovchinnikov, R. K. (2025). Superoxide dismutase activity in tear fluid and blood of patients and mouse model of amyotrophic lateral sclerosis: a pilot study. *PeerJ*, *13*, e19623. https://doi.org/10.7717/peerj.19623

Phattanakiatsakul, T., Chaemsawang, W., Athipornchai, A., Thongon, N., & Chamniansawat, S. (2024). Celastrus paniculatus seed extract exhibits neuroprotective effects against MPP(+)-induced apoptotic cell death via GSK-3β in a Parkinson's disease model. *Biomed Rep*, *20*(3), 46. https://doi.org/10.3892/br.2024.1734

Qian, L., Cui, M., Wu, M., Song, B., Wang, P., Wu, M., He, T., Zhang, B., & He, Y. (2026). Tea-derived natural nanodrug simultaneously enables real-time fluorescent tracking and noninvasive treatment of neuroinflammation in Alzheimer's disease. *J Nanobiotechnology*, *24*(1). https://doi.org/10.1186/s12951-026-04642-5

Ralta, A., Prakash, A., Kumar, M. P., Kumar, R., Sarma, P., Bhatia, A., Medhi, B., & Chakrabarti, A. (2023). Neuroprotective Effect of Celastrus Paniculatus Seed Extract on Epilepsy and Epilepsy-associated Cognitive Deficits. *Basic Clin Neurosci*, *14*(1), 155-166. https://doi.org/10.32598/bcn.2021.3154.1

Ri, M. H., Ri, U. S., Han, H. U., Ko, S. Y., Kim, N. H., Jang, K. S., Kim, K. I., & Sin, Y. S. (2022). Ab initio study of superoxide dismutase (SOD) and catalase activity of EUK-134. *J Mol Model*, *28*(6), 168. https://doi.org/10.1007/s00894-022-05129-4

Rodkin, S., Gasanov, M., Tushev, A., Belousova, E., Gordeeva, Y., Nwosu, C., & Tolmacheva, A. (2026). The Dual Role of Connexins in Stroke, Neurotrauma, Neurodegenerative and Psychiatric Disorders: A Global Systematic Review. *Molecules*, *31*(8). https://doi.org/10.3390/molecules31081341

Satam, S., Raut, S., Shetty, Y. C., Marathe, P. A., Mulkalwar, A., Raut, A., & Rege, N. (2025). Effect of Celastrus paniculatus on Alcohol-Elicited Conditioned Place Preference and Alcohol Withdrawal-Induced Anxiety in Mice. *Cureus*, *17*(4), e81962. https://doi.org/10.7759/cureus.81962

Schwarthoff, S., Tischer, N., Sager, H., Schätz, B., Rohrbach, M. M., Raztsou, I., Robaa, D., Gaube, F., Arndt, H. D., & Winckler, T. (2021). Evaluation of γ-carboline-phenothiazine conjugates as simultaneous NMDA receptor blockers and cholinesterase inhibitors. *Bioorg Med Chem*, *46*, 116355. https://doi.org/10.1016/j.bmc.2021.116355

Shcheblykina, O. V., Kostina, D. A., Pokrovskii, M. V., & Korokin, M. V. (2026). Neurotrophic Factors in Stroke, Traumatic Brain Injury, and Neurodegeneration: A Convergent Pathophysiological and Translational Perspective. *J Integr*

Neurosci, *25*(7), 51543. https://doi.org/10.31083/jin51543

Stefanis, C., Stavropoulou, E., Giorgi, E., Voidarou, C. C., Constantinidis, T. C., Vrioni, G., & Tsakris, A. (2023). Honey's Antioxidant and Antimicrobial Properties: A Bibliometric Study. *Antioxidants (Basel)*, *12*(2). https://doi.org/10.3390/antiox12020414

Tan, B., Suluhan, S. N., Yaylalı, O., Güneş, M. S., & Dursun, N. (2026). Curcumin protects SH-SY5Y cells against glutamate-induced excitotoxicity by maintaining genomic integrity and antioxidant balance. *Drug Chem Toxicol*, 1-10. https://doi.org/10.1080/01480545.2026.2712041

Thongon, N., Phattanakiatsakul, T., & Chamniansawat, S. (2026). Enhancement of Memory and Synaptic Plasticity by Celastrus paniculatus Seed Extract: Upregulation of pSer831-GluA1 Trafficking and Arc/PSD-95 Expression in the Hippocampus of Male Rats. *ScientificWorldJournal*, *2026*, 5390307. https://doi.org/10.1155/tswj/5390307

Tolmacheva, A. S., Sedykh, S. E., Onvumere, M. K., Timofeeva, A. M., Maksimenko, L. V., Gashnikova, N. M., & Nevinsky, G. A. (2024). Catalase Activity of IgG and κκ-IgG, λλ-IgG, and κλ-IgG Subfractions in HIV-Infected Patients and Healthy Donors. *Front Biosci (Landmark Ed)*, *29*(5), 191. https://doi.org/10.31083/j.fbl2905191

Toyokawa, M., Yasuda, K., Kikuya, A., Asada-Utsugi, M., Hida, M., Nakamura, Y., Yanagida, N., Toda, S., Kaji, S., Kinoshita, Y., Ono, Y., Takahashi, R., Matsumoto, R., Kinosita, A., & Maki, T. (2026). Amyloid-β1-42 oligomers compromise oligodendrocyte precursor cells and disrupt blood-brain barrier integrity in vitro. *Brain Res*, *1888*, 150436. https://doi.org/10.1016/j.brainres.2026.150436

van Meerloo, J., Kaspers, G. J. L., & Cloos, J. (2011). Cell sensitivity assays: The MTT assay. *Methods in Molecular Biology*, *731*, 237-245.

Wang, L., Jiang, L., Wang, J., Tang, W., Wang, Z., Guo, R., & Zhang, D. (2025). Reduced glutathione ameliorates sepsis-induced acute kidney injury in mouse model: involvement of cuproptosis. *Ren Fail*, *47*(1), 2518227. https://doi.org/10.1080/0886022x.2025.2518227

Ye, Y., Chen, A., Li, L., Liang, Q., Wang, S., Dong, Q., Fu, M., Lan, Z., Li, Y., Liu, X., Ou, J. S., Lu, L., & Yan, J. (2022). Repression of the antiporter SLC7A11/glutathione/glutathione peroxidase 4 axis drives ferroptosis of vascular smooth muscle cells to facilitate vascular calcification. *Kidney Int*, *102*(6), 1259-1275. https://doi.org/10.1016/j.kint.2022.07.034

Zedde, M., Piazza, F., & Pascarella, R. (2025). Mechanisms of Dural Involvement in Cerebral Amyloid Angiopathy. *Cells*, *15*(1). https://doi.org/10.3390/cells15010026

Zhao, K., Situ, Q. Y., Wang, M., Zhu, H. H., Zhao, H. Y., He, J. H., Tang, Q., Zhang, Y. B., Pei, K. H., Sun, H., & Wang, G. C. (2026). Isoquinoline Alkaloids From Fibraurea recisa With Anti-acetylcholinesterase Activity. *Chem Biodivers*, *23*(1), e03015. https://doi.org/10.1002/cbdv.202503015

Zhao, X., & He, Z. (2025). Traumatic brain injury and Alzheimer's disease related neurodegenerative diseases: Insights from animal models.

Neurosci Res, *221*, 104979. https://doi.org/10.1016/j.neures.2025.104979